

## KINETIC ASPECTS OF THE CRYSTALLIZATION OF SAPO-5 MOLECULAR SIEVES\*

Jan KORNATOWSKI<sup>a,b</sup>, Beate KANZ-REUSCHEL<sup>c</sup>, Gerd FINGER<sup>d</sup>,  
Werner H. BAUR<sup>a</sup>, Martin BÜLOW<sup>d</sup> and Klaus K. UNGER<sup>c</sup>

<sup>a</sup> Institut für Kristallographie und Mineralogie,

J. W. Goethe-Universität, D(W)-6000 Frankfurt/Main, Germany

<sup>b</sup> On leave from Instytut Chemii, Uniwersytet M. Kopernika, PL-87-100 Toruń, Poland

<sup>c</sup> Institut für Anorganische und Analytische Chemie,

J. Gutenberg-Universität, D(W)-6500 Mainz, Germany

<sup>d</sup> Zentralinstitut für Physikalische Chemie, D(O)-1199 Berlin, Germany

Received September 13, 1991

Accepted October 14, 1991

The kinetics of hydrothermal crystallization of microporous silicoaluminophosphate SAPO-5 have been studied as a function of water content using the templates tripropylamine (TPA) and triethylamine (TEA). The investigation included the formation of the SAPO-5 phase, its growth in large single crystals, and the size distribution of the crystals. An attempt to fit the experimental data to kinetic models of crystallization is presented. The systems studied have been found to be very similar except for the nucleation stage which is mainly responsible for both the dimensions of the resulting crystals and for the purity of the SAPO-5 phase.

Microporous aluminophosphates and their derivatives<sup>1</sup> continue to be regarded as promising materials for both scientific and technical purposes<sup>2</sup> and therefore are still being investigated intensively<sup>3-4</sup>. In addition to research into their catalytic properties, studies of materials of AFI topology have been pursued mainly in three directions: 1. methods of synthesis and related problems<sup>2,4-17</sup>; 2. synthesis of large crystals<sup>8-17</sup>; and 3. new derivatives<sup>18-21</sup>. The procedures for synthesis are well developed. Likewise, the growth of large crystals and the tailoring of the dimensions of the crystals have been treated recently<sup>2,15</sup>. However, there are still unsolved problems with regard to phase purity and to the broad size distribution of the crystals<sup>9-16</sup>. These shortcomings can be better solved by gaining a deeper insight into both the kinetics and the mechanisms of the process of crystallization. Only few papers<sup>6,7</sup> deal with the kinetics of crystallization of aluminophosphate molecular sieves and they restrict themselves to the formation of these phases without considering crystal growth.

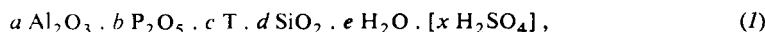
\* Presented as a poster at the *International Symposium "Zeolite Chemistry and Catalysis"*, Prague, September 8-13, 1991.

On the basis of previous work on the SAPO-5 system<sup>14-17</sup>, we have studied the kinetics of the crystallization of this molecular sieve with regard to both the crystallinity of the samples and the dimensions of the crystals as it depends on the water content of the system and on the compounds used to form the reacting gel. Triethylamine (TEA) and tripropylamine (TPA) were applied as templating agents, the latter expected to yield a purer aluminophosphate phase according to refs<sup>6-8</sup>. A comparison of the crystal growth in the systems yielding a pure SAPO-5 phase and the same contaminated by byproducts was accepted by us as an important step for gaining a better insight into the mechanism of crystallization.

Using the equations published earlier<sup>7,22,23</sup>, we tried to fit the time dependence of the crystallization of the SAPO-5 phase in the presence of TPA. We also attempted to interpret the size distribution curves.

## EXPERIMENTAL

Hydrothermal crystallization of SAPO-5 molecular sieves was carried out starting with gels of the formal molar composition



where T = template (TPA or TEA),  $a = 1$ ,  $b = 1$ ,  $c = 1.55$  or  $3.1$ ,  $d = 0.2$ ,  $e = 300$  to  $1\,000$ ,  $x = 0$  for  $c = 1.55$  and  $x = 0.85$  for  $c = 3.1$ . We used orthophosphoric acid as the source of phosphorus, Pural SB (pseudoboehmite) and  $\text{Al}(\text{OH})_3$  sol (pseudoboehmite-like<sup>2</sup>) as the sources of aluminium, Aerosil 380 and Ludox AS 40 as the sources of silicon, and sulfuric acid (96%). The gels were prepared following the commonly used methods and the details are given elsewhere<sup>14-17,24</sup>. Crystallization was carried out at  $190^\circ\text{C}$  under autogeneous pressure without agitation in 50 ml PTFE vessels enclosed in steel autoclaves.

For each kinetic series several autoclaves were charged with the same gel. After appropriate periods of heat treatment (see Results), the autoclaves were cooled down, the products were filtered, washed, and dried at  $110^\circ\text{C}$  for 24 h.

The degree of crystallinity (defined as the amount of SAPO-5 crystallized at a given time) of the samples was determined<sup>6,7</sup> by X-ray powder diffraction and the dimensions of the crystals were measured under a light microscope<sup>25</sup>. The morphology of the crystals was investigated by SEM.

## RESULTS AND DISCUSSION

The system  $\text{Al}_2\text{O}_3 \cdot \text{P}_2\text{O}_5 \cdot \text{SiO}_2 \cdot \text{TPA} \cdot \text{H}_2\text{O}$  containing Pural SB as the aluminium source yields fully crystalline products composed of a nearly homogeneous population of hexagonal prisms of SAPO-5 (Figs 1, 2). Their maximum length along the  $c$ -axis (later called dimension) is shown below in Fig. 12. The X-ray diffractograms of the products correspond exactly to those of crystals of AFI topology and the samples are usually pure. Sometimes a very low content of impurities, namely the  $\text{AlPO}_4$  analogs of cristobalite and tridymite, is present. The formation of these byproducts

is not systematically dependent on changes in synthesis conditions. The characteristics of the usually inhomogeneous products of the TEA containing system have been described elsewhere<sup>14-17,26</sup>.

The  $^{29}\text{Si}$  MAS NMR spectrum as well as the DRIFT (diffuse reflectance infrared Fourier transform) spectrum of the products of the TPA containing system (examples for calcined samples are shown in Figs 3 and 4, respectively) show a predominant incorporation of silicon in the phosphorus sites of the framework. This is similar to what was found in the system containing TEA<sup>14,26,27</sup> and identifies the products as SAPO-5.

The morphology of the crystals grown in the TPA containing system (Figs 1 and 2) shows that:

a) the aspect ratio (length/width) of the crystals increases with water content (dilution) in the reacting gel and this agrees with previous observations for systems containing TEA<sup>2,13-15</sup>;

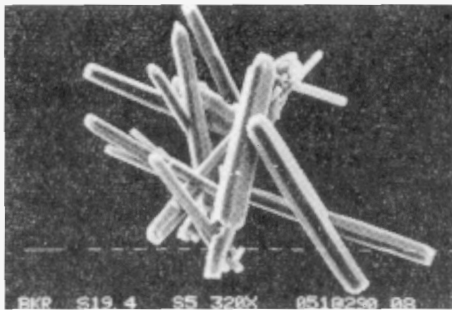


FIG. 1

Crystalline phases of SAPO-5 obtained from the TPA containing system at  $\epsilon = 1000$  [Eq. (1)], 1 bar  $\approx 10 \mu\text{m}$

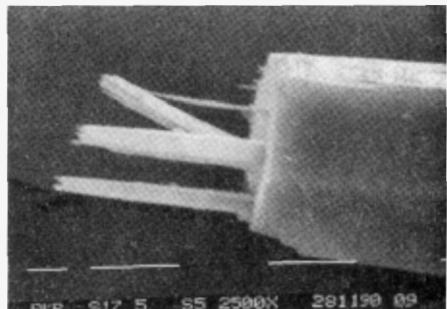
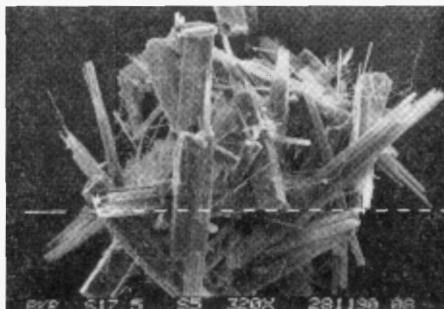


FIG. 2

Epitaxial overgrowing of SAPO-5 crystals (TPA containing system,  $\epsilon = 300$  [Eq. (1)], 1 bar  $\approx 10 \mu\text{m}$ )

b) the crystals (especially at a lower dilution of the reacting gel) are partially overgrown epitaxially along the *c*-axis by thin needles of the same material (Fig. 2). A similar phenomenon has been observed for the system containing TEA but only at higher contents of  $\text{SiO}_2$  in the reacting gel<sup>15,27</sup>. This shows an important role of small  $\text{SiO}_2$  additives in the gel chemistry and/or the crystal growth, particularly because of the observation that the largest SAPO-5 crystals can be grown at an  $\text{SiO}_2$  content of 0.3 mol (ref.<sup>15</sup>).

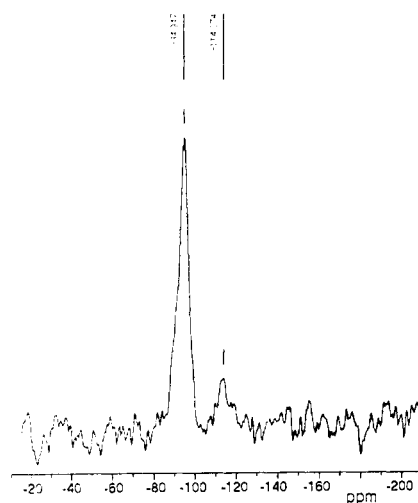


FIG. 3  
Characteristic example for  $^{29}\text{Si}$  MAS NMR of a calcined SAPO-5 sample grown in the TPA containing system (compare ref.<sup>26</sup> for the TEA containing system)

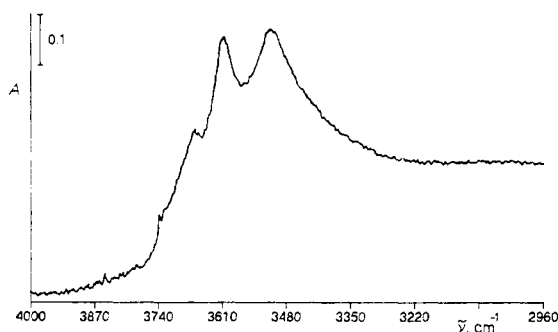


FIG. 4  
Characteristic example for DRIFT spectrum of calcined SAPO-5 sample grown in the TPA containing system (compare ref.<sup>26</sup> for the TEA containing system)

The kinetics of TPA-SAPO-5 crystal growth is illustrated in Fig. 5. The length of the period necessary for reaching full crystallinity (as determined from the surface area of the X-ray peaks)<sup>6,7</sup> increases linearly with the dilution of the reacting gel (Fig. 6). The shape of the kinetic curves depends on the dilution of the system as well, and it is changing from a seemingly linear steep slope at the beginning of the crystallization process to an S-shaped curve indicating an "induction" period<sup>28</sup> for the diluted gel (Fig. 5). A very similar shape of the kinetic curves can be observed for the TEA containing system with the only difference that the yield of SAPO-5 is lower. The S-shaped curve with a very sharp jump is especially well pronounced

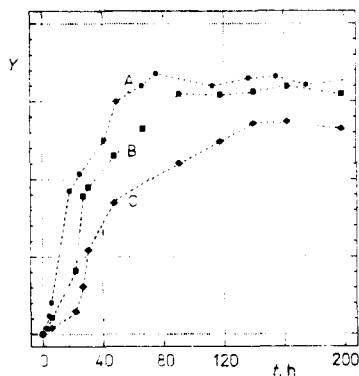


FIG. 5

Kinetics of SAPO-5 crystallization in the TPA containing system. Degree of crystallinity as the function of time at different water contents. A  $e = 300$ , B  $e = 500$ , C  $e = 1000$  [Eq. (1)], Y in arbitrary units

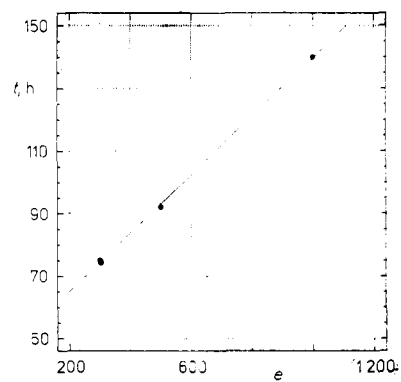


FIG. 6

The period of time necessary for maximum crystallinity of SAPO-5 samples in the TPA containing system as a function of water content (dilution)  $e$  [Eq. (1)]

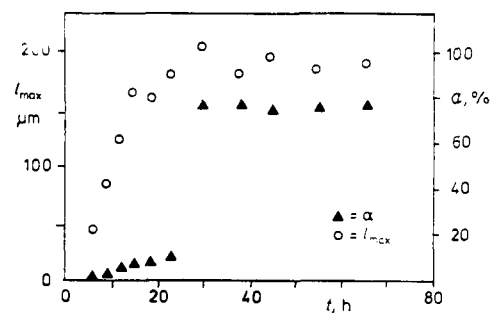


FIG. 7

Kinetics of SAPO-5 crystallization in the TEA containing system at  $e = 750$  and  $c = 3,1$  [Eq. (1)]: ▲ degree of crystallinity ( $\alpha$ ) and ○ maximum crystal length ( $l_{\max}$ ) as functions of time

when an excess of the template is applied (Fig. 7). We conclude that:

- a) the formation of the SAPO-5 phase (without paying any attention to the dimensions of the crystals) is relatively rapid, while its beginning is defined by the gel composition and particularly by the dilution (Figs 5 and 7);
- b) the growth of the crystals (with respect to dimensions) is a relatively quick process (Fig. 7);
- c) the growth of SAPO-5 crystals to large dimensions (up to tens and hundreds of  $\mu\text{m}$ ) is possible only during the initial period of slow increase in crystallinity connected obviously with a slow nucleation rate. The rapid increase of the formation of the SAPO-5 phase results from an acceleration of the nucleation process and/or from reaching the critical size<sup>28</sup> of the nuclei. This is in agreement with the conclusions reached from considering the size distribution of the crystals (see below).

We attempted to fit the experimental kinetic data to the equations

$$K = kt^n \quad (2)$$

proposed by Ceric<sup>22</sup> and Zhdanov<sup>23</sup> and

$$K = 1 - \exp(-(kt)^n) \quad (3)$$

proposed by Weyda and Lechert<sup>7</sup>, where:  $K$  is crystallinity,  $t$  reaction time,  $k$  crystal growth rate,  $n$  pseudo-reaction order.

Since Eq. (2) cannot reflect the levelling off of the crystallization process, the fitting of the experimental data has been restricted up to a crystallinity of about 50%. The results for both models described by Eqs (2) and (3) are given in Table I together with the squares of the correlation coefficients ( $r^2$ ).

In both cases the growth rate  $k$  decreases and  $n$  increases with the dilution of the system. The second model offers a better fitting, though it does not reflect the change

TABLE I  
Crystallization parameters calculated from Eqs (2) and (3) and the squares of the correlation coefficients  $r^2$  for the TPA containing system

Water content [Eq. (1)]	Eq. (2)			Eq. (3)		
	$k$	$n$	$r^2$	$k$	$n$	$r^2$
300	$9.97 \cdot 10^{-3}$	1.395	0.99	$3.859 \cdot 10^{-2}$	1.186	0.99
500	$4.2 \cdot 10^{-4}$	2.136	0.96	$2.582 \cdot 10^{-2}$	1.305	0.98
1 000	$2.3 \cdot 10^{-7}$	4.204	0.98	$1.743 \cdot 10^{-2}$	1.506	0.98

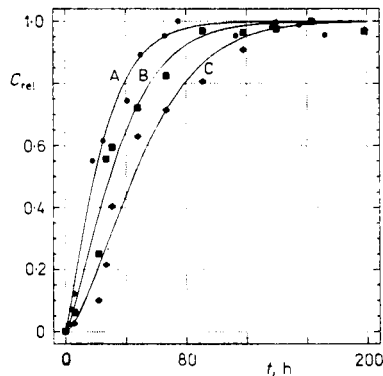


FIG. 8

Relative crystallinity of SAPO-5 samples  $C_{\text{rel}}$  in the TPA containing system as a function of time: experimental values (points — compare Fig. 6) and their fitting to Eq. (3). Lines A, B and C for  $e = 300, 500$  and  $1\,000$  in Eq. (1), respectively

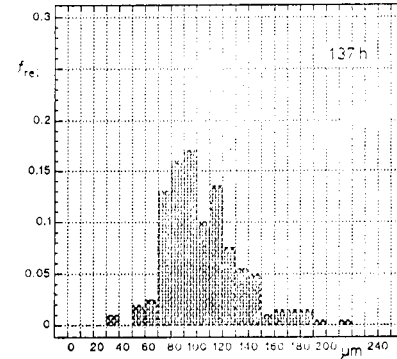
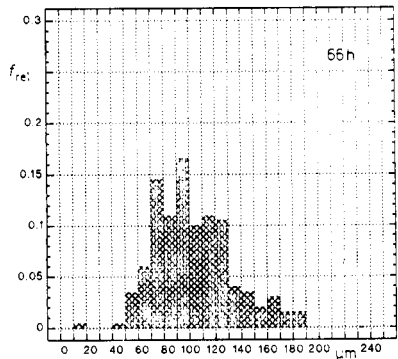
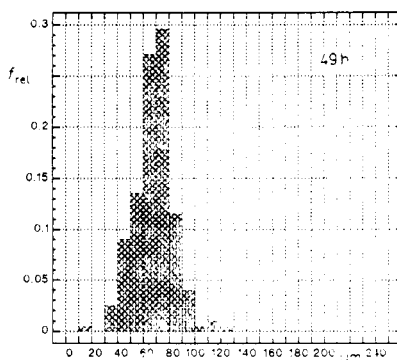
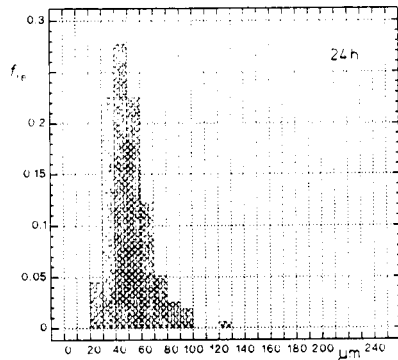


FIG. 9

Size distribution of crystals (dependence of relative frequency  $f_{\text{rel}}$  on particle size in  $\mu\text{m}$ ) of SAPO-5 in the TPA containing system as a function of crystallization time:  $e = 300$  [Eq. (1)]

of the shape of the crystallization curve to an S-curve. Examples of the kinetic curves for the TPA containing system [Eq. (3)] are shown in Fig. 8.

Size distributions of the crystals are presented in Fig. 9 (system with TPA, dilution 300) and in Fig. 10 (system with TEA, dilution 600). Both illustrations have the same character irrespective of the different gel components and the dilutions employed. Their shape is reminiscent of probability distribution curves, except for the tail extended in the direction of larger crystals. The curves shift with time in a regular way towards ever larger crystals until the point at which the most rapid growth of SAPO-5 ends (that is until the end of the most steep part of the kinetic curve is reached). Then the size distribution curves start to broaden but only in the direction of larger crystals. The coincidence of shifting and broadening shows that the nucleation process is stopped which can be caused by large changes in the composition of the reacting gel and/or by competitively rapid formation of the SAPO-5 phase. The last step of the growth of crystals (reflected by a broadening of the size distribution curve) proceeds due to the consumption of the remainders of material present in the mother liquor. One can not exclude a further growth of larger crystals at the expense of the smallest crystals. This broadening of the size distribution curve results obviously in a decrease of its maximum. These conclusions are reinforced by the plot of maximum of the size distribution curves against time (Fig. 11) indicating that both, TPA and TEA containing system undergo the same mechanisms of crystal growth.

However, the relationship between the largest crystal dimensions and the dilution of the reacting gel show a considerable difference between the two systems (Fig. 12). The dilution causes a much stronger increase in the crystal dimensions for the TEA than for the TPA containing system. This may suggest different mechanisms of nucleation in both systems which can be concluded as well from the longer initial period of slowly increasing crystallinity in the first system (Figs 5 and 7, and refs<sup>14,15</sup>). This might be the reason why in the TEA containing system certain byproducts can form<sup>14,15,27</sup> and why their amount is increasing with dilution: the dilution, due to a slowing-down of the nucleation rate, enables the SAPO-5 crystals to grow larger but simultaneously it allows the formation of byproducts to become a more and more competitive process. In the TPA containing system, even at a dilution of 1 000, the nucleation rate remains rapid enough to avoid the formation of any byproducts but, at the same time, it inhibits the growth of larger SAPO-5 crystals.

## CONCLUSIONS

The composition and especially the dilution of the reacting gel are important factors in the growth of SAPO-5 crystals. The content of SiO<sub>2</sub> influences markedly the

morphology of the crystals. The nucleation rate decreases with the dilution of the system. The formation of the SAPO-5 phase and the growth of individual crystals

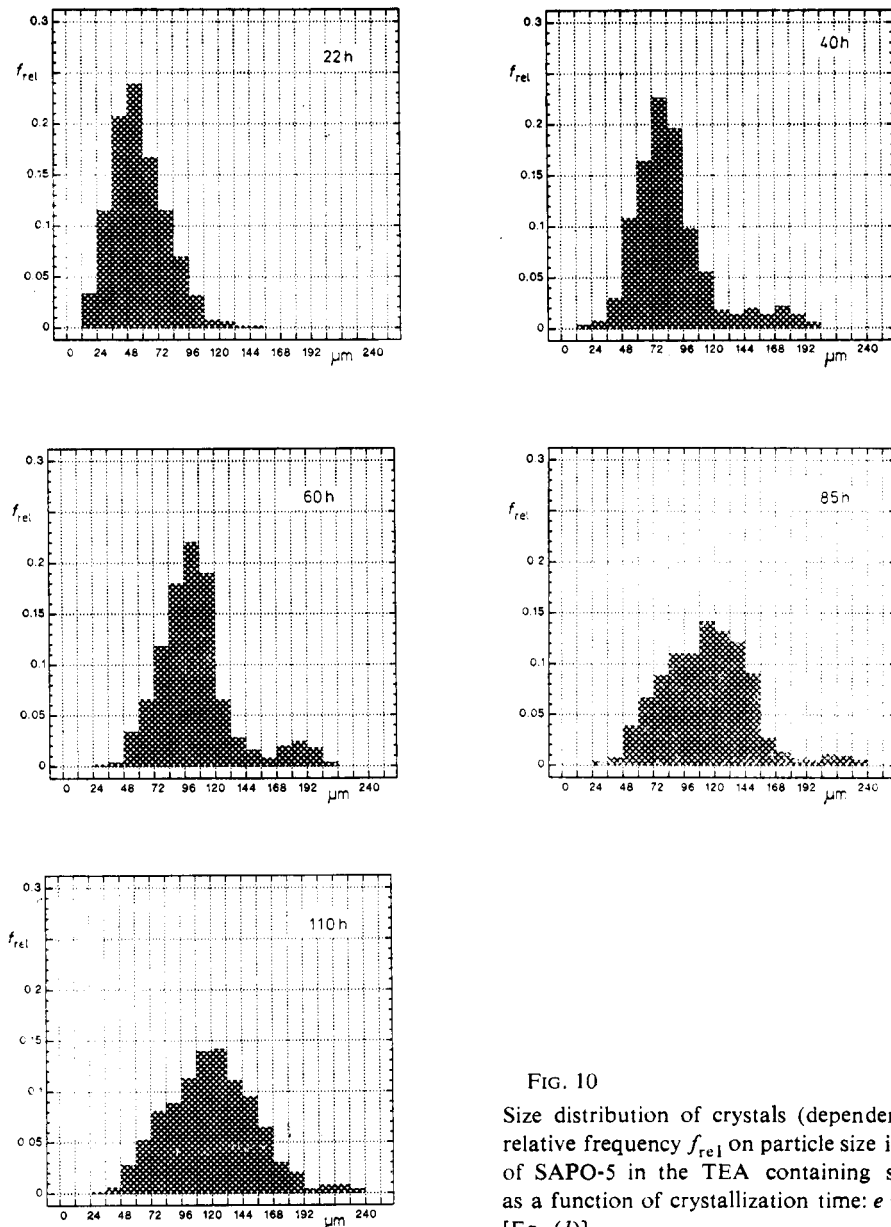


FIG. 10  
Size distribution of crystals (dependence of relative frequency  $f_{\text{rel}}$  on particle size in  $\mu\text{m}$ ) of SAPO-5 in the TEA containing system as a function of crystallization time:  $e = 600$  [Eq. (1)]

(the dimensions of which depend on the number of nuclei) proceed rapidly. At the end of the rapid formation of the SAPO-5 phase, the nucleation process is stopped and the rest of unreacted gel is consumed for a further growth of crystals already formed. This causes a broadening of the size distribution curve. The formation of byproducts depends on the relationship between the competitive nucleation rates of SAPO-5 and the byproducts. Though both systems investigated differ in the composition of the reacting gel, the mechanisms of SAPO-5 crystal growth are similar except for a different nucleation process. In the TPA containing system, the SAPO-5 phase is obtained solely but the system is less sensitive to dilution and therefore very large crystals do not grow. In contrast, the TEA containing system

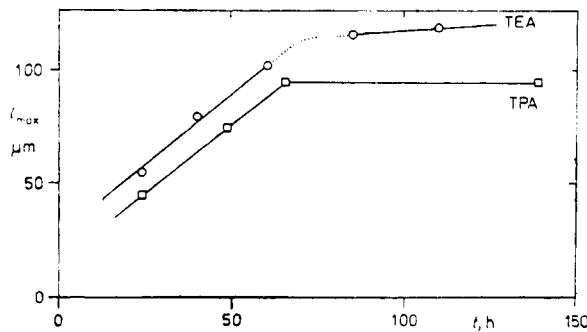


FIG. 11

Maxima of the size distribution curves ( $l_{\max}$  (Figs 9 and 10) as a function of time for TEA and TPA templates

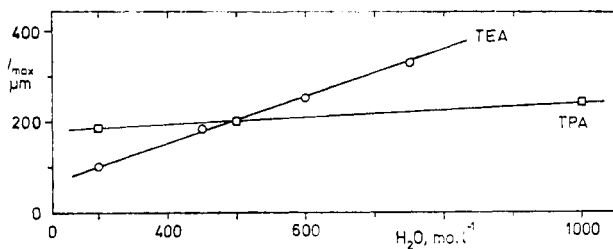


FIG. 12

Maximum crystal length ( $l_{\max}$ ) as a function of water content in the gel at  $c = 1.55$  [Eq. (1)] for TEA and TPA templates

is able to yield larger crystals but the sample is always contaminated by byproducts in amounts increasing with the size of the crystals (with dilution).

*The work was supported by the Bundesministerium für Forschung und Technik, the Polish Committee for Scientific Research (KBN), and the AIF fund of DECHEMA.*

## REFERENCES

1. Flanigen E. M., Lok B. M., Patton R. L., Wilson S. T.: *Stud. Surf. Sci. Catal.* 28, 103 (1986); *Pure Appl. Chem.* 58, 1351 (1986).
2. Finger G., Richter-Mendau J., Bülow M., Kornatowski J.: *Zeolites* 11, 443 (1991), and refs 1, 4—6 therein.
3. Flanigen E. M., Patton R. L., Wilson S. T.: *Stud. Surf. Sci. Catal.* 37, 13 (1988).
4. Ren X., Komarneni S., Roy D. M.: *Zeolites* 11, 142 (1991).
5. Jahn E., Müller D., Wieker W., Richter-Mendau J.: *Zeolites* 9, 177 (1989).
6. Weyda H., Lechert H. in: *DECHEMA-Monographien*, Vol. 118, p. 159. VCh-Verlagsgesellschaft, Weinheim 1989.
7. Weyda H., Lechert H.: *Zeolites* 10, 251 (1990).
8. Shilun Qiu, Wenqin Pang, Kessler H., Guth J.-L.: *Zeolites* 9, 440 (1989).
9. Müller U., Unger K. K.: *Z. Kristallogr.* 182, 190 (1988).
10. Müller U., Brenner A., Reich A., Unger K. K.: *ACS Symp. Ser.* 398, 347 (1989).
11. Finger G., Kornatowski J., Bülow M., Rozwadowski M.: *Ger. DD* 286,564 (1991).
12. Kornatowski J., Rozwadowski M., Finger G., Bülow M.: *Pol. Appl. P* 280,471 (1989).
13. Kornatowski J., Finger G.: *Bull. Soc. Chim. Belg.* 99, 857 (1990).
14. Finger G., Kornatowski J.: *Zeolites* 10, 615 (1990).
15. Finger G., Kornatowski J., Richter-Mendau J., Jancke K., Bülow M., Rozwadowski M.: *Stud. Surf. Sci. Catal.* 65, 501 (1991).
16. Finger G., Kornatowski J., Jahn E., Bülow M., Rozwadowski M., Zibrowius B.: *Ger. DD* 285,765 (1991).
17. Kornatowski J., Rozwadowski M., Finger G., Jahn E., Bülow M., Zibrowius B.: *Pol. Pat. Appl. P* 280,470 (1989).
18. Van Nordstrand R. A., Santilli Don S., Zones S. I.: *ACS Symp. Ser.* 368, 236 (1988).
19. Iton L. E., Choi I., Desjardins J. A., Maroni V. A.: *Zeolites* 9, 535 (1989).
20. Wilson S. T., Flanigen E. M.: *ACS Symp. Ser.* 398, 329 (1989).
21. Kornatowski J., Finger G.: Unpublished results.
22. Ceric J.: *J. Colloid Interface Sci.* 28, 315 (1968).
23. Zhdanov S. P.: *Adsorbenty*, p. 10. Nauka, Leningrad 1978.
24. Kanz-Reuschel B.: *Thesis*. 1991.
25. Beyer H., Riesenbeck H.: *Handbuch der Mikroskopie*, 3. Auflage, pp. 401—408. VEB Verlag Die Technik, Berlin 1988.
26. Zibrowius B., Löffler E., Finger G., Sonntag E., Hunger M., Kornatowski J.: *Stud. Surf. Sci. Catal.* 65, 537 (1991) and refs 7, 11—17 therein.
27. Finger G., Jahn E., Zeigan D., Zibrowius B., Szulzewsky K., Richter-Mendau J., Bülow M.: *Bull. Soc. Chim. Belg.* 98, 291 (1989).
28. Warzywoda J., Edelman R. D., Thompson R. W.: *Zeolites* 9, 87 (1989).